Monitoring the dynamics of a coherent cavity polariton population

J. Bloch,* B. Sermage, M. Perrin, and P. Senellart
LPN/CNRS, Route de Nozay, 91460 Marcoussis, France

R. André and Le Si Dang
LSP/CNRS, Université J. Fourier, Grenoble, BP 87, 38402 St Martin d'Hères, France
(Received 17 December 2004; revised manuscript received 28 January 2005; published 13 April 2005)

We report on time-resolved photoluminescence measurements on a II-VI CdTe/CdMnTe semiconductor microcavity in the strong-coupling regime. Under nonresonant excitation, we observe the buildup of a large population in the polariton states close to the Brillouin-zone center with occupation factors larger than 10. A spectacular spectral narrowing is measured, together with a strong acceleration of the polariton relaxation. A simple rate equation model describing the stimulated polariton-polariton scatterings toward the lowest-energy polariton states gives a good overall description of the measured dynamic.

DOI: 10.1103/PhysRevB.71.155311 PACS number(s): 78.47.+p, 78.45.+h, 71.36.+c

Semiconductor microcavities in the strong-coupling regime[1] have attracted a lot of interest these last years because they appear as good candidates to study the bosonic nature of excitons and observe an analogous to a Bose condensation in a solid-state system.[2,3] Indeed, in microcavities containing quantum wells, the eigenstates are mixed exciton-photon states (polaritons) whose in-plane dispersion relation close to $k_{\|}=0$ is extremely steep compared to the bare quantum well.[4] As a result, polariton dispersion relations exhibit a deep trap in energy close to the Brillouin-zone center (in-plane wave vector $k_{\|}=0$). When quasiresonantly creating polaritons in this energy trap, stimulated polariton-polariton scattering can be triggered as well as polariton amplification,[5–7] giving rise to correlated polariton pairs.[8]

Even more interesting is the possibility of obtaining such a large accumulation of polaritons at the bottom of the trap under nonresonant excitation. In III-V microcavities, under highly nonresonant excitation, the strong-coupling regime is bleached before a significant polariton population can be achieved in the trap.[9–11] The polariton dispersion is so steep that the relaxation from large-$k_{\|}$ states toward the bottom of the trap through both acoustic phonon and polariton-polariton scattering is inhibited.[12]

The situation is different in II-VI microcavities: several groups have reported stimulated scattering both under nonresonant excitation[13–16] and in a pump-probe experiment with a nonresonant pump.[17,18]

In this work, we use time-resolved photoluminescence (PL) to study the dynamics of the buildup of a large polariton population in the polariton trap under nonresonant excitation. We observe a sharp threshold in excitation power above which the emission is superquadratic, its dynamics accelerates, and a pronounced spectral narrowing is observed. We directly measure the polariton occupation factors at $k_{\|}=0$ and find that it is close to unity at threshold in agreement with the framework of polariton-stimulated scattering. We show that simultaneously to the nonlinear growth of the polariton population close to $k_{\|}=0$, the population at large $k_{\|}$ is clamped above threshold. Finally we develop a simple model based on rate equations which describes the evolution of the polariton population both as a function of time and excitation power. It gives a good overall picture of the system dynamics both for $k_{\|}=0$ states and large-k states.

Our sample consists in a 2λ $Cd_{0.4}Mg_{0.6}Te$ microcavity containing four 8-nm CdTe quantum wells and surrounded by two $Cd_{0.4}Mg_{0.6}Te/Cd_{0.75}Mg_{0.25}Te$ Bragg mirrors. The top (bottom) mirror contains 17.5 (23) pairs. At resonance between the exciton and cavity mode, we measure a Rabi splitting of 10.5 meV. The sample is maintained at 10 K (lattice temperature). The excitation is delivered by a pulsed Ti:sapphire laser providing 1.5-ps pulses with a 12-ns repetition time and focused on the sample with a spot diameter of 50 μm. Its energy is tuned to the first reflectivity minimum above the mirror stop band, around 100 meV above the polariton energy. The emission is collected through a small diaphragm (defining an angular aperture of 3°) selecting an emission direction θ. Thus we measure the emission of polaritons with a given in-plane wave vector $k_{\|}$ with $k_{\|}=k_0\sin(\theta)$ [k_0 is the wave vector of the emitted light (in air)].[4] The emission is spectrally dispersed and temporally analyzed with a streak camera. The spectral resolution is 0.2 meV. For some measurements, we obtain a time resolution of 10 ps by masking part of the monochromator grating with a slit parallel to the grooves.

We choose a point on the sample corresponding to detuning close to zero ($\delta=1$ meV) between the exciton and cavity photon mode under normal incidence ($k_{\|}=0$). Polaritons at $k_{\|}=0$ are half matter-half light states. Figure 1(a) presents PL spectra recorded at different time delays after the excitation pulse for an excitation power P of 0.4 mW. The lower polariton line peaks at 1.627 eV with a linewidth of 3 meV. The emission dynamics is slow: it reaches maximum 100 ps after the laser pulse. Actually within the considered time window, the onset of the emission decay is barely seen. As shown in Fig. 1(b), the dynamics is drastically changed for $P=1.5$ mW. The emission peak arises around 70 ps after the laser pulse and its intensity is more than two orders of magnitude larger than for $P=0.4$ mW. Moreover the emission spectrum for time delays close to 70 ps presents a pronounced spectral narrowing.

Since above threshold the maximum PL signal is reached

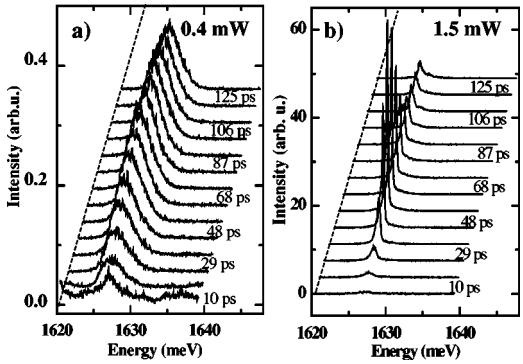

FIG. 1. PL spectra at $k_{\|}=0$ measured at different time delays after the excitation pulse for (a) $P=0.4$ mW and (b) $P=1.5$ mW. Spectra have been vertically and horizontally shifted for clarity. Vertical arbitrary units in (a) and (b) are the same.

after 70 ps, we can monitor the polariton dispersion at very short time delays just after the laser pulse. To do so, we probe the emission dynamics for several external angles and study the emission energy at very short time delays, typically 20 ps after the excitation pulse. Figure 2(a) shows the energy dispersion measured at short time delays for several excitation powers. At low P, the characteristic polariton trap is evidenced and the energy dispersion is fitted with a 10.5-meV Rabi splitting and $\delta=+1$ meV. Above threshold (for $P=1.4$ mW and 3 mW), the polariton dispersion is modified but the polariton trap is still clearly observed. We fit the energy dispersion with a reduced Rabi splitting of 9.5 meV (6.7 meV) for an excitation power of 1.4 mW (3 mW). Because of the large number of excitons created at short time delays, the exciton oscillator strength is reduced and the Rabi splitting is weakened.[19] Nevertheless, the system remains in the strong-coupling regime just after the laser pulse when the number of carriers in the system is maximum. This proves that it is legitimate to consider polariton eigenstates. On the contrary for $P=6$ mW, we observe a broad nondispersive line. At this excitation power, excitons are bleached and we measure the emission of an electron-hole pair plasma in weak coupling with the cavity mode. At longer time delay, a conventional laser emission by the

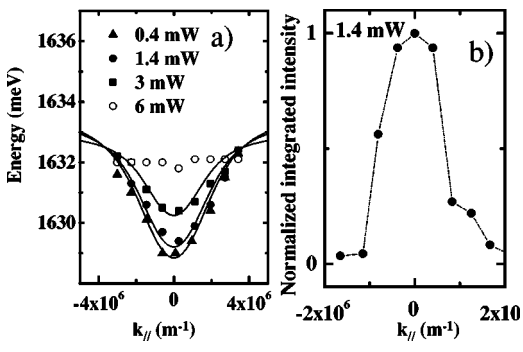

FIG. 2. (a) Symbols: PL peak energy measured at short time delays (20 ps after the laser pulse) as a function of $k_{\|}$ for various excitation powers. Solid lines: calculated dispersion relations with a Rabi splitting of 10.5, 9.5, and 6.7 meV. (b) Integrated intensity measured as a function of $k_{\|}$ for a 1.4 mW excitation power.

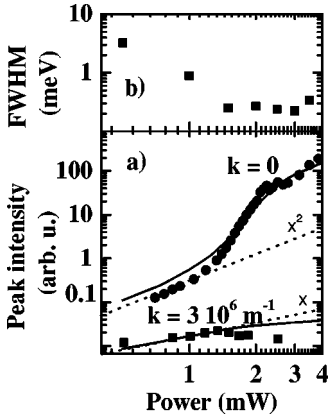

FIG. 3. (a) Circles (squares): peak intensity measured for $k_{\|}=0$ ($k_{\|}=310^6$ m^{-1}) as a function of the excitation power. Solid lines: calculated peak intensities as a function of the excitation power for $k_{\|}=0$ and $k_{\|}=3\times10^6$ m^{-1}. (b) Spectral full width at half maximum measured in $k_{\|}=0$ at the time delay corresponding to the peak intensity.

electron-hole plasma is observed. Surprisingly, at high excitation powers we do not observe the cavity mode line for short time delays. This is probably due to the fact that the system is filled with electron-hole pairs: the cavity mode cannot establish because of a too strong free carrier absorption. We could observe the cavity mode at high excitation powers for more negative detunings, a configuration where the absorption at the cavity mode energy is reduced.

We now study the power dependence of the polariton emission. Figure 3(a) summarizes the peak intensity (spectrally integrated) measured both in $k_{\|}=0$ and at large in-plane wave vector ($k_{\|}=3\times10^6$ m^{-1}). Below threshold, a quadratic increase of the intensity is observed at $k_{\|}=0$, a signature of polariton-polariton scattering. The nonresonant excitation mainly creates polaritons in the reservoir of large $k_{\|}$ states. Because of the steep polariton dispersion close to $k_{\|}=0$, polariton scattering via acoustic phonons is not efficient and polariton relaxation is governed by polariton-polariton scattering.[20] Above 1 mW, a strong nonlinearity occurs at $k_{\|}=0$: the signal increases by more than two orders of magnitude when doubling the excitation power. The behavior of the emission at large $k_{\|}$ is drastically different. Since the polariton states at $k_{\|}=3\times10^6$ m^{-1} are at the edge of the polariton trap and close in energy to the reservoir states, they are well coupled to the reservoir of large-k states via acoustic phonon scattering. Therefore their emission directly reflects the reservoir population. At low excitation power, it increases linearly with the excitation power whereas above threshold it is clamped. This indicates that the nonlinear emission we observe is the result of an efficient transfer of polaritons from the reservoir toward the bottom of the polariton trap. Finally, the $k_{\|}=0$ nonlinearity is associated with an abrupt spectral narrowing of the polariton line as shown in Fig. 3(b). The $k_{\|}=0$ polariton linewidth goes down to 0.2 meV, below the bare cavity linewidth ($\simeq$1.2 meV). This is the signature of the appearance of a temporal coherence[21] in the system with a coherence time larger than 3 ps.

To further demonstrate the buildup of a large polariton

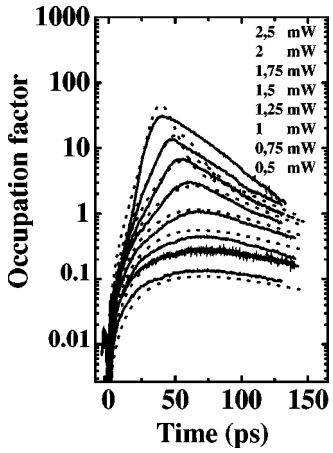

FIG. 4. Solid lines: occupation factor measured at $k_{\|}=0$ as a function of time for various excitation powers. Dashed lines: calculated occupation factors as a function of time for the same excitation conditions. The laser arrival time lies close to $t=0$.

population close to $k_{\|}=0$, we directly deduce from the absolute PL intensity the polariton occupation factor. To do so, we have calibrated our experimental setup to convert detector units into watts and adapt the method described in Ref. 9 to a pulsed excitation. Within the 50-μm-diam spot on the sample and the experimental angular aperture of radius $\delta k = 2.6\times10^5$ m^{-1}, we measure the emission of 20 polariton states. To deduce the occupation factor, we only need the cavity lifetime, which can be measured at large negative detuning under resonant excitation.[22] In this sample, this lifetime is below temporal resolution: we estimate $\tau_c=0.5$ ps from the PL linewidth at large negative detunings. Figure 4 shows the time evolution of the lower polariton occupation factor as a function of time for different excitation powers. The strong increase of the emission close to $k_{\|}=0$ occurs when the polariton occupation factors become close to unity. Above threshold we measure an occupation factor larger than 10. In this regime, the emission dynamics changes: the rise time becomes continuously smaller and the emission peak progressively occurs at shorter time delays. This change in the dynamics together with the measurement of large occupation factors proves the onset of a stimulated scattering mechanism.

The emission in k space is shown in Fig. 2(b) with a maximum at $k_{\|}=0$ and a $1/e$ half width of 10^6 m^{-1}. At $k_{\|} = \pm10^6$ m^{-1}, the energy of the narrow line is blueshifted by 0.1 meV with respect to $k_{\|}=0$. This energy dispersion is characteristic of the polariton dispersion. Thus, the stimulated scattering gives rise to a large polariton population on all polariton states within $k_{\|}\leqslant10^6$ m^{-1}. This corresponds to approximately 300 polariton states. We therefore observe a transient large occupation factor of several hundreds polariton states close to $k_{\|}=0$ under highly nonresonant excitation.

Let us calculate the polariton relaxation dynamics. A simple rate equation model is used with three manifolds: (i) polaritons close to $k_{\|}=0$ with an occupation factor $f_p(t)$ and a number of states $\mathcal{N}_p$ [the total polariton population is given by $n_p(t)=\mathcal{N}_P f_p(t)$], (ii) polaritons in the reservoir of large-$k_{\|}$ states with a total population $n_R(t)$ and a number of states $\mathcal{N}_R$, and (iii) high-energy excitons with a population $n_H(t)$ [the nonresonant pump creates high-energy electron-hole pairs which relax into manifold (iii) via optical phonon interaction]. This latter manifold is introduced in the model to describe the signal rise time, governed by the relaxation rate between the high-energy exciton states [manifold (iii)] and the reservoir of cold excitons [manifold (ii)].

We only consider exciton-exciton scattering and neglect acoustic phonon scattering since even at low P, the emission is quadratic with P. The time evolution of the three population manifolds is governed by the following rate equations:

$$\frac{dn_H}{dt} = Q(t) - A\mathcal{N}_R n_H, \tag{1}$$

$$\frac{dn_R}{dt} = A\mathcal{N}_R n_H - \frac{n_R}{\tau_R} - \alpha_{exciton}^2 B n_R^2 \mathcal{N}_P(1+f_p), \tag{2}$$

$$\frac{dn_p}{dt} = -\frac{n_p(1-\alpha_{exciton}^2)}{\tau_{cav}} + \alpha_{exciton}^2 B n_R^2 \mathcal{N}_P(1+f_p). \tag{3}$$

$\alpha_{exciton}$ is the polariton exciton part and Q the pump rate proportional to P. Considering a 1% absorption per quantum well, $Q(t)=8\times10^5\,\delta(t)$ polaritons injected in manifold (iii) for $P=500$ μW. Coefficient A describes the relaxation rate from manifold (iii) to (ii); B describes scattering of two polaritons from the reservoir resulting in the transfer of one polariton into $k_{\|}=0$ and another back in the reservoir [manifold (ii)]. We do not consider any stimulation or Pauli blocking in manyfolds (ii) and (iii): due to their large density of states, the occupation factors in manyfolds (ii) and (iii) always remain far below unity.

At low excitation power, because of the relaxation bottleneck,[12] the emission in $k_{\|}=0$ state simply reflects the dynamics of excitons in the reservoir. The emission rise time reflects the relaxation time from high-energy excitons toward the excitonic reservoir whereas the decay time reflects the mean recombination time of the excitonic reservoir. Therefore, by fitting the emission dynamics at low P, we can deduce both A and τ_R. We find $(A\mathcal{N}_R)^{-1}=30$ ps and $\tau_R = 200$ ps. The absolute value of the occupation factor of the $k_{\|}=0$ manifold below threshold fixes the amplitude of the polariton-polariton scattering coefficient: we find $B=0.3$ s^{-1}. This coefficient is close to the theoretically predicted polariton-polariton scattering rates.[20,23] According to these references, with a spot size of 50 μm, $B=0.2$ s^{-1}. Finally, the only parameter left to be determined is $\mathcal{N}_P$, the number of polariton states on which the stimulated scattering occurs. This parameter controls the amplitude of the nonlinear increase of the polariton population above threshold. If $\mathcal{N}_P = 1$, this amplitude is huge, much larger than experimentally observed. When increasing N_P, polaritons are distributed on a larger number of polariton states, thus limiting the population of each polariton state and therefore the term $(1+f_p)$ in Eq. (3). As a result, the acceleration of the stimulated scattering and the amplitude of the nonlinearity are reduced. The best fit to the experimental data is obtained for $\mathcal{N}_P=2000$ polariton states.

We can now calculate the time evolution of the polariton

population both in $k_{\|}=0$ and large-k states for various excitation power. The calculated peak intensities are plotted in Fig. 3(a). The model describes both the increase of the polariton population close to $k_{\|}=0$ and the saturation of the reservoir population above threshold. The calculated decay curves are shown in Fig. 4 for $k_{\|}=0$. The main features in the dynamics are well reproduced in particular, the progressive shortening of the rise time as the polariton population builds up. This shortening is due to the acceleration of the relaxation induced by the large occupation factor in manifold (i) [second term in Eq. (3)]. Let us underline that the occupation factors used in the calculations are exactly equal to the measured occupation factors. Neither the experimental curves nor the calculated ones in Fig. 4 have been vertically shifted to obtain the observed agreement between theory and experiment. Finally, we notice that at the highest P, the calculated decay of the $k_{\|}=0$ population is much shorter than experimentally observed and presents a biexponential decay. The shorter decay comes from the abrupt emptying of the polariton reservoir induced by the fast-stimulated scattering into manifold (i). Even though the reservoir population is experimentally clamped, its dynamics does not reflect this transient depletion. Indeed our three-manifold model cannot account for the complexity of scattering mechanisms occurring within the reservoir: some reservoir states are emptied by the stimulated scattering whereas others are not affected and contribute to repopulate the latter. The emptying of these reservoir states limits experimentally the amplitude of the nonlinear growth of the $k_{\|}=0$ population. This probably explains why we have to introduce in the model a stimulated scattering over 2000 polariton states and not over 300 as estimated experimentally. If we consider a stimulated scattering over 300 polariton states, the calculated nonlinearity is too strong as compared to the experiment.

Finally, our measurements show that the relaxation time between the high-energy states resonant to the pump energy and the reservoir of cold excitons is as short as 30 ps. This is in great contrast to III-V microcavities where similar measurements evidence a much slower relaxation rate with a time constant of the order of 150 ps (Ref. 24). Thus, in II-VI compounds, exciton cooling is much more efficient probably because of a stronger interaction with optical phonons. This may explain why stimulated scattering under nonresonant excitation can be achieved in II-VI compounds as opposed to GaAs-based III-V microcavities.

To conclude, we have observed under nonresonant excitation the buildup of a large polariton population in the polariton states close to $k_{\|}=0$. Their emission presents a strong spectral narrowing above threshold. In this stimulated scattering regime, the population of the polariton states at larger $k_{\|}$ is clamped, evidencing the stimulated transfer from large-k states to $k_{\|}=0$ states. We developed a simple rate equation model, allowing us to get an overall understanding of the stimulation dynamics. In particular, the model indicates that the shorter thermalization time of the exciton like reservoir, due to a stronger exciton LO-phonon interaction, could be the key parameter explaining why stimulated scattering is observed in II-VI microcavities and not in III-V.

We thank Guillaume Malpuech for fruitful discussions. This work was partly supported by the "Région Ile de France" and the "Conseil Général de l'Essonne."

*Electronic address: jacqueline.bloch@lpn.cnrs.fr

[1] C. Weisbuch, M. Nishioka, A. Ishikawa, and Y. Arakawa, Phys. Rev. Lett. **69**, 3314 (1992).

[2] For a review see M. Scholnick, A. I. Tartakovskii, R. Butté, R. M. Stevenson, J. J. Baumberg, and D. M. Whittaker, in *Nano-Optoelectronics*, edited by M. Grundmann (Springer-Verlag, Berlin, 2002).

[3] Fabrice P. Laussy, G. Malpuech, A. Kavokin, and P. Bigenwald, Phys. Rev. Lett. **93**, 016402 (2004).

[4] R. Houdré, C. Weisbuch, R. P. Stanley, U. Oesterle, P. Pellandini, and M. Ilegems, Phys. Rev. Lett. **73**, 2043 (1994).

[5] P. G. Savvidis, J. J. Baumberg, R. M. Stevenson, M. S. Skolnick, D. M. Whittaker, and J. S. Roberts, Phys. Rev. Lett. **84**, 1547 (2000).

[6] R. M. Stevenson, V. N. Astratov, M. S. Skolnick, D. M. Whittaker, M. Emam-Ismail, A. I. Tartakovskii, P. G. Savvidis, J. J. Baumberg, and J. S. Roberts, Phys. Rev. Lett. **85**, 3680 (2000).

[7] M. Saba, C. Ciuti, J. Bloch, V. Thierry-Mieg, R. André, Le Si Dang, S. Kundermann, A. Mura, G. Bongiovanni, J. L. Staehli, and B. Deveaud, Nature (London) **414**, 731 (2001).

[8] S. Savasta, O. Di Stefano, V. Savona, and W. Langbein, cond-mat/0411314v1 (unpublished).

[9] P. Senellart, J. Bloch, B. Sermage, and J. Y. Marzin, Phys. Rev. B **62**, R16 263 (2000).

[10] A. I. Tartakovskii, M. Emam-Ismail, R. M. Stevenson, M. S. Skolnick, V. N. Astratov, D. M. Whittaker, J. J. Baumberg, and J. S. Roberts, Phys. Rev. B **62**, R2283 (2000).

[11] R. Butté, G. Delalleau, A. I. Tartakovskii, M. S. Skolnick, V. N. Astratov, J. J. Baumberg, G. Malpuech, A. Di Carlo, A. V. Kavokin, and J. S. Roberts, Phys. Rev. B **65**, 205310 (2002).

[12] F. Tassone, C. Piermarocchi, V. Savona, A. Quattropani, and P. Schwendimann, Phys. Rev. B **56**, 7554 (1997).

[13] Le Si Dang, D. Heger, R. André, F. Boeuf, and R. Romestain, Phys. Rev. Lett. **81**, 3920 (1998).

[14] F. Boeuf, R. André, R. Romestain, Le Si Dang, E. Péronne, J. F. Lampin, D. Hulin, and A. Alexandrou, Phys. Rev. B **62**, R2279 (2000).

[15] M. D. Martin, G. Aichmayr, L. Vina, and R. André, Phys. Rev. Lett. **89**, 077402 (2002).

[16] M. Richard, J. Kasprzak, R. André, Le Si Dang, and R. Romestain, J. Phys.: Condens. Matter **16**, S3683 (2004).

[17] A. Alexandrou, G. Bianchi, E. Péronne, B. Hallé, F. Boeuf, R. André, R. Romestain, and Le Si Dang, Phys. Rev. B **64**, 233318 (2001).

[18] R. Huang, Y. Yamamoto, R. André, J. Bleuse, M. Muller, and H. Ulmer-Tuffigo, Phys. Rev. B **65**, 165314 (2002).

[19] R. Houdré, J. L. Gibernon, P. Pellandini, R. P. Stanley, U. Oesterle, C. Weisbuch, J. O. Gorman, B. Roycroft, and M. Ilegems, Phys. Rev. B **52**, 7810 (1995).

[20] F. Tassone and Y. Yamamoto, Phys. Rev. B **59**, 10 830 (1999).

[21] J. J. Baumberg, P. G. Savvidis, P. G. Lagoudakis, M. D. Martin, D. Whittaker, R. Butté, M. Skolnick, and J. Roberts, Physica E (Amsterdam) **389**, 13385 (2002).
[22] B. Sermage, S. Long, I. Abram, J. Y. Marzin, J. Bloch, R. Planel, and V. Thierry-Mieg, Phys. Rev. B **53**, 16 516 (1996).
[23] D. Porras, C. Ciuti, J. J. Baumberg, and C. Tejedor, Phys. Rev. B **66**, 085304 (2002).
[24] J. Bloch, B. Sermage, C. Jacquot, P. Senellart, and V. Thierry-Mieg, Physica E (Amsterdam) **390**, 390 (2002).